CASSINI ION AND NEUTRAL MASS SPECTROMETER OBSERVES ORGANIC MOLECULES IN THE UPPER ATMOSPHERE OF SATURN. K. E. Miller[1], J. H. Waite, Jr.[1], R. Perryman[1], C. R. Glein[1], M. Perry[2], and D. Mitchell[2], [1]Southwest Research Institute, San Antonio, TX, [2]Johns Hopkins Applied Physics Laboratory, Laurel, Maryland, USA, 20723. Correspondence to kmiller@swri.edu.

Introduction: The Cassini spacecraft was in orbit in the Saturnian system from 2004 until 2017. During that time, the Ion and Neutral Mass Spectrometer (INMS) collected compositional data from the atmosphere of Titan [1, 2], the plume of Enceladus [3], and ring particles [4]. At the close of the Grand Finale, Cassini skimmed within 1800 km of Saturn five times before its final plunge into Saturn. Throughout these final six revolutions, INMS collected *in situ* data. The resulting mass spectra record a complex zoo of organic species up to at least the mass 99 limit of INMS in addition to the expected H_2 and He. The altitude-density profiles of these species are found to be consistent with an external flux of material into Saturn's upper atmosphere near the equator.

Previous studies have indicated the presence of "ring rain" – material influxing from the rings into Saturn's atmosphere with a pronounced effect on the ionosphere at low latitudes [5, 6]. Grand Finale data from the Cassini Charge-Energy-Mass Spectrometer (CHEMS) instrument suggest that the equatorial influx of material includes heavy nanoparticles (10,000-40,000 amu), which are detected along the path of the proximal orbits [7]. If organic, these nanoparticles would be expected to fragment in the INMS closed source antechamber, given the 31 km s^{-1} speed difference between the Cassini spacecraft and Saturn's equatorial atmosphere. Here, we present compositional data from INMS of the ring rain region, with the goal of understanding which compounds are fragments of the nanoparticles and which compounds are volatile constituents derived from the D ring.

Dataset: We focus our analyses on the subset of INMS closed source data from Revolutions (hereafter, Rev.) 288 through 292 below 1800 km (referenced to the 1 bar level). These data have lower statistical noise because of the increased count rates at higher pressures, while still providing a range of altitudes over which to analyze the behavior of different detected masses. (The minimum altitude reported is 1644 km from Rev. 291.) We exclude Rev. 293 at present because of data analysis complications that arise from the truncation of the orbit.

Analyses:

Composition. Preliminary compositional assignments for the spectra are made using a combination of INMS calibrated reference spectra and National Institute of Standards and Technology (NIST) reference spectra to determine the electron impact fragmentation patterns. These NIST spectra provide a reasonable approximation to INMS [2]. The fitting routine [2] scales the primary peak (typically but not necessarily the molecular ion) for a species of interest to the corresponding mass in the spectrum, and produces a residual spectrum by subtracting the resulting fragment counts from fragment peaks. Since fitting one mass affects the residual signal for all associated fragment masses, the order in which species are added is important. For Rev. 288, we fit the spectrum from high masses to low masses to account for this dependence. Fits for Rev. 291 and 292 were produced by independently scaling each species from Rev. 288 in the same order. For each revolution, a subset of data between 1700 and 1800 km was utilized.

Flux continuity. Based on the compositional fits, we assigned the dominant contributor for five high signal peaks: mass 15 (CH_4), mass 28 (preliminary assignment is CO [4, 8], though the fits for CO and N_2 are degenerate and C_2H_4 may contribute), mass 44 (CO_2), mass 58 (C_4H_{10}), and mass 78 (C_6H_6). The altitude-dependent count rates for these species follow the same distribution as the H_2 density, suggesting that the particle velocity is limited by diffusion.

Flux continuity requires that the product of the particle velocity and density should be constant as a function of altitude. Assuming negligible thermal diffusion, the maximum velocity is given as $w = (D/H)*(1-m_1/m)$, where D is the diffusion coefficient (a function of particle mass and radius), H is the scale height, m_1 is the particle mass, and m is the average atmospheric mass [9]. We performed a linear fit to the density-altitude and velocity-altitude profiles and iteratively solved for the derived particle radius that resulted in slopes with the same magnitude, consistent with flux continuity. These derived radii were compared to radii in the literature for the molecular species to attribute each mass to molecular species or fragments of larger particles. Fits were also performed for mass 91 and for a theoretical particle with a mass of 10,000 amu. The density profile for the 10,000 amu particle used data from mass 58.

Correlations. The correlation of counts for different masses provides an independent test of their association in the upper atmosphere. To first order, volatile species should correlate closely with one another, and the products of ring rain fragmentation should be sepa-

rately correlated. We calculated the Pearson correlation coefficient for the weighted mean of data binned by time at nine different masses (15, 18, 28, 44, 51, 56, 70, 78, and 91), and checked for patterns in the correlation coefficients for different pairings.

Results:

Composition. As expected, the dominant species by mixing ratio for all three revolutions analyzed were H_2 and He. Excluding these species, the remainder is dominated by organics, including CH_4. The compositions of the three revolutions are comparable to one another, although Rev. 291 appears to be more water-rich than the other two orbits.

Flux continuity. The derived particle radii required to match flux continuity constraints are shown as a function of mass in Fig. 1. For masses 15 and 28, the radii are < 1 nm. Masses 44, 58, 78, and 91 have calculated radii between 1 and 10 nm, while the radius for a particle mass of 10,000 amu is > 10 nm.

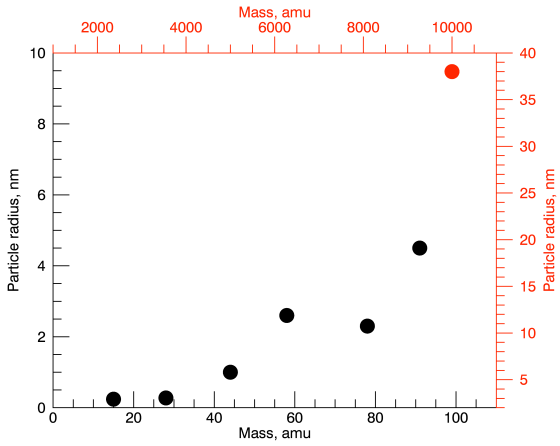

Correlations. A strong correlation ($R^2 \geq 0.95$) was observed in all revolutions for mass 15 and mass 28, mass 15 and mass 44, and mass 28 and mass 44. Correlations with higher masses were not consistent across revolutions.

Discussion: The INMS proximal orbit dataset reveals an influx of heavy organic species into Saturn's atmosphere from an external source, consistent with ring rain. The complexity in the composition of the ring rain is completely unexpected. The composition of the different revolutions is similar, but some variation is present. This variation may reflect differences in the spacecraft track relative to Saturn and possibly localized sources of ring rain ("storms" of ring rain). Rev. 291 stands out as an end-member orbit in these analyses in terms of the number of correlated species as well as the density of water and organic species.

The calculated particle radii for masses 15 and 28 are consistent with the molecular radii for methane and carbon monoxide respectively [10]. (The radius for mass 28 does not rule out N_2 or C_2H_4.) The relatively large calculated radii for heavier species may indicate that they are fragments associated with the breakup of organic nanoparticles in Saturn's exosphere and/or within the INMS closed source antechamber [11]. (The molecular radius for benzene, for example, is approximately 0.3 nm [10], nearly an order of magnitude less than the calculated ~2 nm). This conclusion is generally supported by the strong correlation of masses 15, 44, and 28. The lack of consistent correlation between heavier masses may indicate spatial variation in fragmentation or dissociation of the nanoparticles.

Acknowledgements: This work was supported by the INMS subcontract from JPL to the Cassini INMS science team.

References: [1] Waite J. H. *et al.*, (2005) *Science, 308*, 982-986. [2] Magee B. A. *et al.*, (2009) *Planetary and Space Science, 57*, 1895-1916. [3] Waite J. H. *et al.*, (2006) *science, 311*, 1419-1422. [4] Perry M. E. *et al.*, (2010) *Journal of Geophysical Research: Space Physics, 115*. [5] Moore L. *et al.*, (2015) *Icarus, 245*, 355-366. [6] O'Donoghue J. *et al.*, (2013) *Nature, 496*, 193-195. [7] Mitchell D. G. *et al.*, (2017) *AGU*, Abstract [8] Noll K. S. *et al.*, (1986) *The Astrophysical Journal, 309*, L91-L94. [9] Banks P. M., Kockarts G., *Aeronomy*. (Academic Press, 1973). [10] *Tables of Physical & Chemical Constants (16th edition 1995). 2.2.4 Mean velocity, free path and size of molecules. Kaye & Laby Online. Version 1.0 (2005)* www.kayelaby.npl.co.uk [11] Waite J. H. *et al.*, (2009) *Nature, 460*, 487-490.